

Transmission Line Conductor Temperature Impact on State Estimation Accuracy

Marija Bočkarjova, *Student Member, IEEE*, Göran Andersson, *Fellow, IEEE*

Abstract—State estimation has become a tool of vital importance in modern control centers. If the accuracy of the state estimation could be increased this will mean that a more reliable representation of the power system is obtained and the operation and control functions can make better decisions. This paper studies the influence of changes of the transmission lines resistance due to temperature on state estimation performance. The possibility to account for this effect in state estimation is shown by the use of Line Heat Balance equation and weather data.

Index Terms—Measurement errors, Power system state estimation, Transmission lines, Power transmission meteorological factors.

I. INTRODUCTION

THE secure operation of power system must be ensured by the Control Center operators, and a primary need of the operators is reliable information. Establishment of Supervisory Control And Data Acquisition (SCADA) systems was an important achievement, however data obtained from SCADA may not always be correct containing e.g. measurement or circuit breaker status errors. Moreover, not all the measurements are available in the Control Center.

These concerns were first recognized by Fred Schweppe, who proposed and investigated State Estimation (SE) methods [1] giving the most likely state of power system from possibly limited raw measurement data.

Nowadays, state estimation is an important and a widely used control center tool. It forms the basis for a number of applications, such as:

- System observation
- Security assessment
- Optimal power flow
- Transmission system usage billing.

The performance and reliability of SE is strongly dependent on the accuracy of the defined power system model.

A number of methods has been developed for model parameter verification and estimation, as summarized in [2], [3], [4]. State vector augmentation and the residual analysis methods are addressing estimation of rather limited number of selected parameters, while processing of several sequential snapshots either by the enlarged conventional SE or Kalman filter is more suitable for the multiple erroneous parameter identification. The usefulness and importance of these methods

are indisputable. Particularly, efficient application should be expected in case of relatively large parameter error and its impact on SE and high measurement redundancy. However, less significant deviations may be difficult to distinguish from the measurement errors impact.

Besides the initial errors in databases, some parameters may vary for different operating conditions. Changes in line capacitance due to line sag are small. The resistance of the transmission lines changes significantly with temperature, however it does not deteriorate state estimation performance drastically [2] and have not been previously considered in the models. We believe that further enhancements of SE accuracy, particularly important for the correct transmission losses allocation in nodal pricing markets, can be achieved nowadays when powerful computational capabilities and communication links are available.

This paper considers the impact of transmission lines resistance changes due to line currents and ambient weather conditions on the state estimation accuracy, as well as the possibility to account for these changes.

II. THE THEORETICAL BACKGROUND

A. State Estimation principles

State estimation considers the mapping of the states x to measurements z biased by measurement errors e :

$$\begin{aligned} z_i - h_i(x) &= e \\ x &= (\theta_1 \theta_2 \dots \theta_n U_1 \dots U_n)^T \end{aligned} \quad (1)$$

where $h(x)$, known as *measurement function*, relates the system state vector x containing voltage angles and magnitudes to the measured quantities - voltage magnitudes V_i , bus power injections P_i, Q_i , branch power flows P_{ij}, Q_{ij} .

The measurement errors are assumed stochastic and the following properties of these are usually being assumed: Gaussian probability distribution, zero mathematical expectation values and mutual independence. Therefore, equation (1) can be solved giving the most likely values of the state variables based on the available measurements.

Since the measurement error expectation values have been assumed to be zero, the most likely estimation in this case [1], [4] corresponds to the states minimizing the following objective function:

$$J = \sum_{i=1}^m W_{ii} [z_i - h_i(x)]^2. \quad (2)$$

The weights W_{ii} are inversely proportional to the measurement error variance $W_{ii} = 1/\sigma_i^2$.

This work has been financially supported by ABB Switzerland Ltd., Corporate Research.

M. Bočkarjova and G. Andersson are with Power Systems Laboratory of Swiss Federal Institute of Technology (ETH) in Zürich, Physikstrasse 3, CH-8092 Zürich, Switzerland, e-mails: {bockarjova, andersson}@eeh.ee.ethz.ch.

Minimum of J can be determined using the first order optimality conditions $g(x) = \frac{\partial J(x)}{\partial x} = 0$. Expanding $g(x)$ in Taylor series around $x^{(k)}$ and neglecting the higher order terms, we obtain:

$$g(x^{(k)}) + \frac{\partial g(x^{(k)})}{\partial x}(x - x^{(k)}) = 0. \quad (3)$$

Thus, the Gauss-Newton iterative solution scheme [5] can be employed to find x satisfying (3). Proceeding with rearrangements leads to the formulation known as *Normal equations*:

$$G(x^k)\Delta x^{(k+1)} = H^T(x^{(k)}) \cdot W \cdot [z - h(x^{(k)})], \quad (4)$$

where

- $G(x) = \frac{\partial^2 J(x)}{\partial x^2} = H^T(x) \cdot W \cdot H(x)$ is gain matrix
- $\Delta x^{(k+1)}$ is the update of the solution at iteration k , so $x^{(k+1)} = x^{(k)} + \Delta x^{(k+1)}$
- $H(x) = \frac{\partial h(x)}{\partial x}$ is measurement Jacobian.

Solving this equation for $\Delta x^{(k+1)}$ and iterating until the required accuracy ε is reached, i.e. $\Delta x^{(k+1)} < \varepsilon$, one will obtain the solution of SE.

B. Resistance Dependence on the Temperature

In practise, the conductor temperature varies in the range 0° to $60^\circ C$ or even larger, resulting in changes of the line resistance.

Since the stranding of the conductor has a negligible effect on the ratio of effective to dc resistance [6] and the conductor operates in the temperature range far from the melting point, temperature dependance can be determined as:

$$R_{T1} = R_{T0}[1 + \alpha(T_1 - T_0)] \quad (5)$$

where $\alpha = 0.0039 [C^{-1}]$ is the temperature coefficient for aluminium, R_0 and R_1 are the resistances at temperatures T_0 and T_1 correspondingly.

AC resistance increases due to the skin effect. For even number layered ACSR conductors it can be determined with a good accuracy either by the analytical expressions or through precomputed R_{ac}/R_{dc} curves [6]. For the conductors with odd number of layers, the additional influence of the eddy currents and hysteresis losses in the steel core cannot be neglected and the AC resistance depends on both temperature and the current.

In the following computations, we assume even layered conductors and linear dependance of AC resistance only on the conductor temperature, although nonlinear dependance could be accounted for in the similar manner.

C. Current-Temperature Relationship of a Conductor

The current-temperature relationship of a bare overhead conductor is addressed by IEEE standard [7], which is essentially based on the proposed and investigated by the House and Tuttle method [8]. The overhead line temperature depends on the following conditions:

- Conductor material properties
- Conductor electrical current
- Conductor diameter and surface conditions
- Ambient weather conditions: wind, sun, air.

TABLE I
INPUT PARAMETERS

Parameter	Source
Weather	
V_w	velocity of the air stream, ft/h
ϕ_w	angle between conductor axis and the air stream, deg
T_a	ambient temperature, $^\circ C$
$Q_s(H_c, H_e)$	total solar and sky radiated heat flux, W/ft^2
Atmosphere - weather dependent	
$\rho_f(H_e, T_{film})$	air density, lb/ft^3
$\mu_f(T_{film})$	absolute viscosity of air, $lb/(ft \cdot h)$
$k_f(T_{film})$	air thermal conductivity coefficient, W/ft
Line-Sun layout - location and time dependent	
Z_c	azimuth ¹ of sun, deg
Z_l	azimuth of line, deg
H_c	altitude of the sun, deg
H_e	elevation of conductor above the sea level, ft
Conductor	
D	conductor diameter, in
A'	projected area of conductor, ft^2 per lineal ft
ϵ	emissivity
α	solar absorptivity
R_{T_c}	resistance per lineal foot of conductor at T_c , Ω/ft
SCADA/EMS output	
I	line currents, A

¹ Azimuth is a the horizontal component of a direction - the angle along the horizon, with zero degrees corresponding to North, and increasing in a clockwise fashion [12].

Assuming that changes of the power system state are relatively slow, we employ the steady-state models suggested in [7] for the transmission line resistance correction. The contribution of the mentioned above factors in steady state can be summarized by the Heat Balance equation [8], as follows:

$$I^2 R_{Tc} + q_s = q_c + q_r \quad (6)$$

where I is the conductor current, R_{Tc} is resistance at the temperature T_c , q_c and q_r are the heat losses due to convection and radiation, respectively, q_s is the solar heat gain.

The expressions below determine heat losses and gain, while the input parameters are summarized in table I. The units of measurements indicated in the table correspond to the coefficients in (7) - (9) and adopted from [7].

- The *solar heat* gain can be computed, as:

$$q_s = \alpha Q_s A' \sin \theta \quad (7)$$

where $\theta = \cos^{-1}[\cos(H_c) \cos(Z_c - Z_l)]$. Solar absorptivity α increases with the conductor age depending on the atmospheric pollution and line operating voltage $\alpha = 0.7$ can be used, if the exact value is unknown.

- The *radiated heat* loss is:

$$q_r = 0.138 D \epsilon \frac{(T_c + 273)^4 - (T_a + 273)^4}{100^4}. \quad (8)$$

Similarly to solar absorptivity, emissivity ϵ also increases over the years: $\epsilon = 0.5$ is the approximate value to be used.

- Forced *convection heat loss* at low wind speed is:

$$q_c = K_\phi k_f (T_c - T_a) \left[1.01 + 0.371 \left(\frac{D \rho_f V_w}{\mu_f} \right)^{0.52} \right] \quad (9)$$

where $K_\phi = 1.194 - \cos(\phi) + 0.194 \cos(2\phi) + 0.368 \sin(2\phi)$ is a term that accounts for the angle ϕ

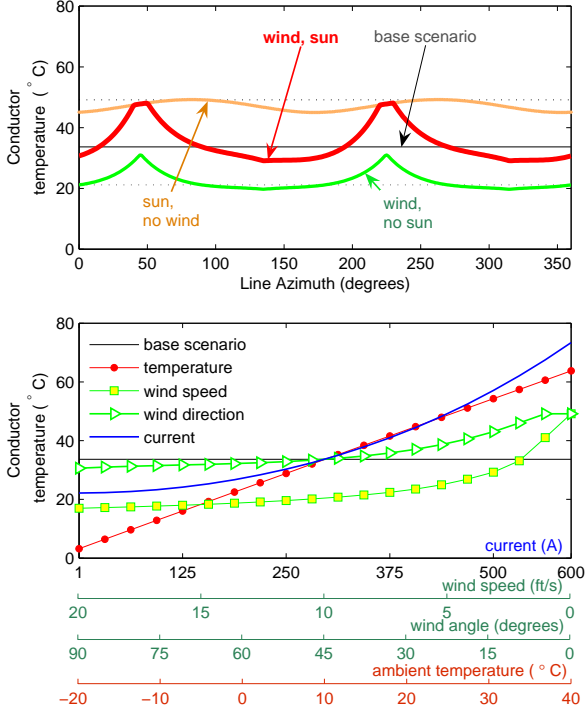


Fig. 1. Influence of the single parameter variation on the conductor temperature

between the wind direction and conductor axis, k_f , p_f , μ_f depend on air film temperature $T_{film} = (T_a + T_c)/2$.

After a more careful consideration of the required parameters one can conclude that input of just four direct measurements is necessary for the application of the method: *wind, air temperature, heat flux and the conductor current*.

Let us consider possible variations of the conductor temperature by changing single parameter in the base scenario determined by the following conditions:

- wind: north-east, $V_w = 2$ ft/s;
- ambient temperature: $T_a = 10^\circ\text{C}$;
- sun: $H_c = 49.0^\circ$, $Z_c = 172.5^\circ$, $Q_s = 91.93$ W/ft² ;
- current: 300 A;
- conductor: 397.500 ACSR 30/7, $D = 0.806$ in, $R_{25^\circ\text{C}} = 0.235$ ohm/mile, $\epsilon = 0.5$, $\alpha = 0.7$, $H_e = 850$ ft, $Z_l = 90^\circ$ west-east direction.

Atmospheric parameters, such as air density are calculated by the approximation formulas provided in [7].

Fig. 1 shows the resulting conductor temperature variations. The upper plot addresses conductor temperature dependence on line azimuth Z_l , which indirectly impacts both the convected heat loss q_c and the solar heat gain q_s . Green and orange curves provided for a comparison evaluate these impacts separately: only angle ϕ_w changes at no sun conditions and only angle θ changes at no wind conditions. While the wind direction has slightly stronger influence than the sun, the combined impact of both parameters may result in approximately 20°C variations of the conductor temperature.

The bottom plots in Fig. 1 demonstrate the influence of the conducted current, ambient temperature, wind speed and direc-

tion on the wire temperature. One of the parameters is varied, while the others are kept constant as in the base scenario. The ambient temperature and the conducted current have a significant impact on the conductor temperature: for the realistic ambient temperature variations in the range $[-20, 40]^\circ\text{C}$ the conductor temperature varies in the chosen conditions from 0 to 60°C . The conductor current was simulated from 0 to maximal conductor current carrying capacity limit of 600A causing 50°C increase. Wind blowing in perpendicular to the transmission line would produce 10°C cooling in comparison to wind blowing in parallel to the conductor. Realistic variation of conductor emissivity and absorptivity have little impact on the final evaluation of the conductor temperature.

The analysis of the temperature variations depending on the operating conditions shows that the variation range can easily exceed 50°C resulting in more than 20% changes of the conductor resistances, according to (5).

The measurements of the weather conditions may contain some error. Fig. 2 considers the influence of these uncertainties by Monte-Carlo simulations for the base scenario above and the increased wind speed $V_w = 5$ ft/s. In addition, it was assumed that the errors are normally distributed $N(\mu, \sigma^2)$, specifically:

- wind speed: $V_w \sim (5, 1)$;
- ambient temperature: $T_a \sim N(10, 1)$;
- sun flux: $Q_s \sim N(92, 5^2)$;
- current: $I \sim N(300, 3^2)$;
- line: $Z_l \sim N(90, 5^2)$, $H_e \sim N(850, 50^2)$;

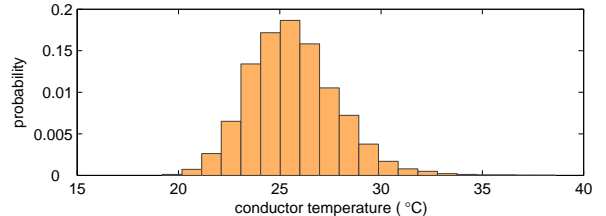


Fig. 2. Probability distribution of the conductor temperature in presence of the parameters uncertainty.

Such uncertainties combinations produce standard error of 2°C (68.2% confidence interval). Thus, the described method of the conductor temperature calculation results in satisfactory accuracy in presence of realistic parameter uncertainty.

III. MODIFICATIONS OF SE ALGORITHM

The classical SE procedure can be modified to account for the discussed effect of the conductor heating in the particular loading and weather conditions.

Fig. 3 shows the diagram of the suggested algorithm. Analog measurements obtained by SCADA are processed by the 1st stage SE, followed by the resistance correction in accordance with estimated current and the weather conditions. The updated power system model is used then at the second stage SE. The system state is not expected to change drastically and the states obtained at the 1st stage seem to be a logical choice for the initial values of the 2nd stage SE. The following step is the decision about necessity to repeat resistance

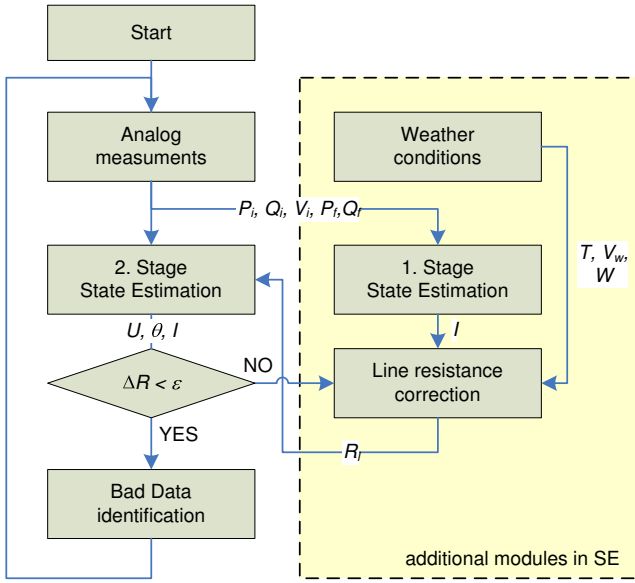


Fig. 3. Proposed state estimation algorithm.

correction for all (or part of) the lines. A small number of iterations is sufficient. The resistance correction may be also performed based on the measured current (recomputed from the flow measurements) values. However, one SE run may be suggested - at least due to possible lack of the necessary measurements in the system.

As an alternative to the algorithm in Fig. 3 that uses inputs for implicit conductor temperature calculations, any other the conductor temperature measurement can be applied. For example, as discussed in [13] line thermal monitoring method based on phasor measurement units (PMU) can be used.

The method described in II-C was preferred for the discussion, as it is suitable for the simulation of thermal processes and is standardized. An additional advantage of this method is that it does not require installation of additional hardware: the weather conditions data can be easily obtained from the meteorological institutions usually having measurement stations at different locations around the country.

IV. SIMULATIONS AND RESULTS

A. Power System Model

The study of the model inaccuracies impact on the SE results was conducted for IEEE 14-bus test system [9]. The single line diagram of the system is shown in Fig. 4.

The system consists of two voltage levels: busses 1-5 are operated at 132kV and busses 6-14 at 33kV. For the higher voltage lines 397.500 ACSR 30/7 conductor is assumed, as for the example in II-C, with 26ft conductor spacing. For the lower voltage level 266.80 ACSR 26/7 conductor at 10ft spacing is assumed having $R_{25^{\circ}C} = 0.350 \text{ ohm/mile}$ and $D = 0.642 \text{ in.}$ Line azimuths are:

$$Z_l = [90, 170, 160, 70, 160, 10, 60, \dots \\ 140, 10, 20, 30, 40, 100, 50, 80].$$

Since the selected test system represents a portion of the real power system in the Midwestern US (in February, 1962),

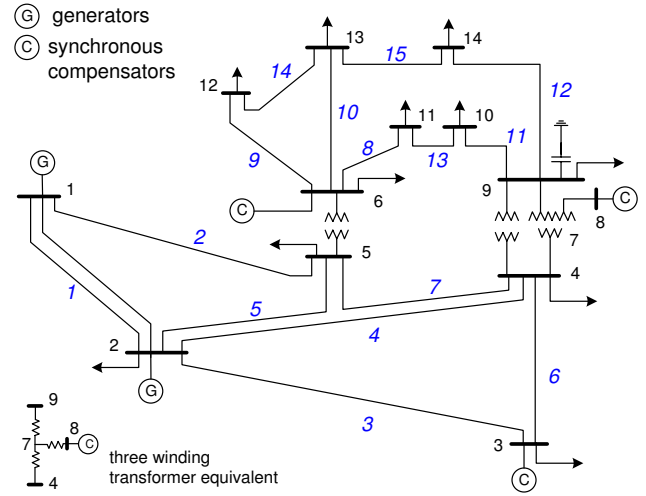


Fig. 4. Single line diagram of the IEEE 14-bus system.

the assumed location is Ohio and the geographical parameters are chosen accordingly: latitude $39^{\circ}08'N$, longitude $84^{\circ}31'W$, $H_e = 850 \text{ ft.}$ Sun position can, thus, be calculated [12].

State estimation includes measurements of all the voltage magnitudes, all active and reactive power injections, as well as all active and reactive power flows. Assumed standard deviation of the measurements errors is $\sigma_U = 1\%$ for the voltage measurements and $\sigma_{pq} = 1.5\%$ for the power flow and injection measurements.

B. Temperature impact on SE accuracy

The impact of a resistance increase by 20% was studied. It corresponds to realistic conductor temperature increase from the regular $20^{\circ}C$ design temperature to allowable $70^{\circ}C$.

In Fig. 5 the actual values of the voltage magnitudes (computed by power flow) are compared with the output of two the state estimators: using power system model for standard design conditions and model adjusted to the actual operating conditions. It can be concluded that for increased conductor temperatures the use of the uncorrected model would result in higher voltage profile than in reality. In case of state estimator based on the correct model, the errors appear due to noise in measurements of electrical parameters.

Fig. 6 shows the residuals of active power flows on the transmission lines. The residuals are the difference between power measurements and the estimated values. In the case of uncorrected system model, the residuals are higher due to

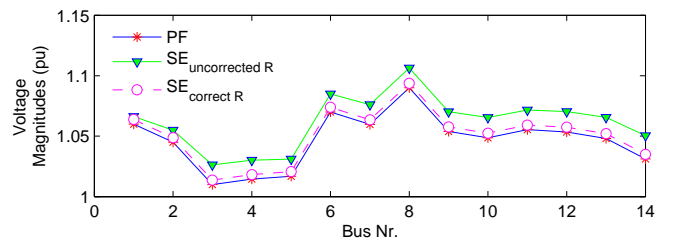


Fig. 5. Voltage magnitudes computed by power flow and estimated.

combined effect of both electrical measurement errors and the additional inaccuracy introduced by the uncorrected values of the line resistances. The latter is at least comparable to the measurement noise impact. Although in some cases, the resistance error "corrects" the measurement noise impact, in the overall the residuals are considerably smaller for corrected transmission model providing higher confidence in the obtained results.

Relative errors of the estimated active power flows compared to the true values (determined by power flow) are shown in Fig. 7:

$$error = \frac{true - estimate}{true} \cdot 100\%.$$

The overestimation of the conducted flows may reach almost 10 % due to neglected temperature impact. In the open market conditions, this might represent financial implications, particularly in presence of congestion.

Moreover, the active power losses are estimated inaccurately in case of the uncorrected line resistance, as shown in Fig. 8. Here, Monte-Carlo simulations were applied to determine distribution of the error in estimated losses: 100 trials of random electrical measurement errors followed by state estimation were conducted and the results were summarized. The expected value of the error and the standard deviation interval are shown. In case of correct model, the expected error in determined losses is zero. In case of use of uncorrected resistances, the underestimated losses may reach 20% for some transmission lines. The total value for the whole system approaches 15%, resulting in incorrect budgeting of the losses to ancillary services instead of being charged to producing companies.

C. SE accuracy variation during 24-hour period

The impact of the conductor heating on SE accuracy may vary for different systems, topologies and states. As an example, we observe the SE accuracy during 24 hour period, for the arbitrary chosen day - October, 1st.

Two accuracy metrics were adopted from [14] to evaluate the performance of SE for both uncorrected and corrected power system models:

- Metric for complex power flow estimation accuracy, as follows:

$$M_{Sflow} = \sqrt{\sum_j \frac{|\vec{S}_{j,from}^{true} - \vec{S}_{j,from}^{est}|^2 + |\vec{S}_{j,to}^{true} - \vec{S}_{j,to}^{est}|^2}{MVA_j^2}}$$

where \vec{S} is complex power in the line j , MVA is the maximum capacity of the line;

- and the voltage accuracy metric:

$$M_V = \|\vec{V}^{error}\|_2 = \sqrt{\sum_j |\vec{V}_j^{true} - \vec{V}_j^{est}|^2}.$$

Constant northern wind $V_w = 2 ft/s$ and following temperature conditions are assumed:

$$hour = [0, 2, 4, 6, 8, 10, 12, 14, 16, 18, 20, 22]$$

$$T_a = [20, 20, 20, 22, 25, 26, 28, 30, 30, 28, 26, 22].$$

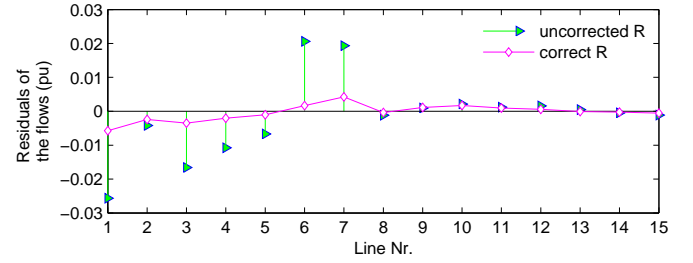


Fig. 6. Residuals of the determined flows.

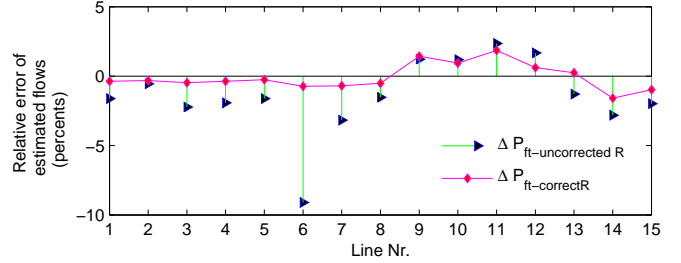


Fig. 7. Relative errors of the determined flows in percents to actual values.

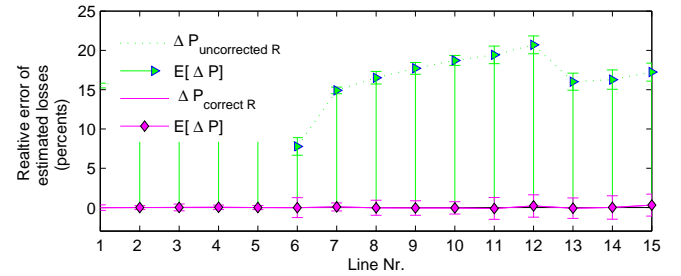


Fig. 8. Expected errors and standard deviations in computed losses.

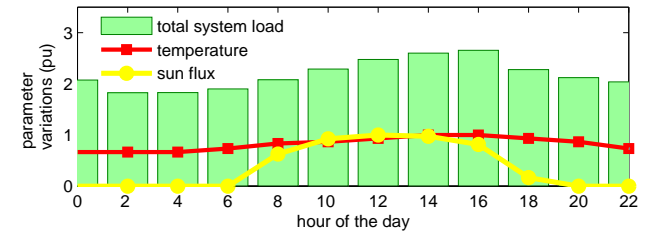
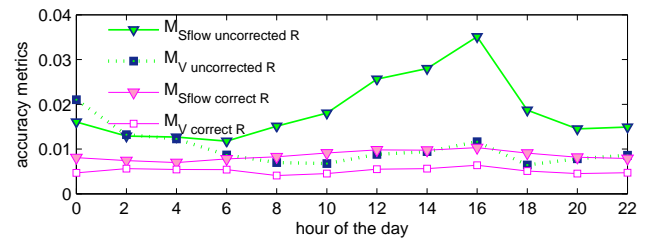


Fig. 9. SE metric variations during 24 hour time period

Loads changes are covered by the slack generator at bus 1. Ratio of bus load to the total the system loading is normally distributed around the value obtained from the initial state [9] with 5 % standard deviation. The total system load is shown in Fig. 9, as well as sun flux and temperature variations normalized to peak values.

The results of the simulations in Fig. 9 show the expected values of the metric during the day at the simulated voltage and power measurement errors. For the comparison, the metric values for more detailed study of 20 % resistance increase (IV-B) are the following:

Metric	Correct Resistance	Uncorrected Resistance
M_{Sflow}	0.0099	0.0538
M_V	0.0053	0.0459

It can be noted that values of these accuracy indices are close to ones at the loading peak in Fig. 9 and the observations from the previous subsection are applicable to both cases.

For the chosen day the highest deterioration of the estimation accuracy M_{Sflow} due to temperature impact on the conductor resistances approximately coincide with the loading peak. Metrics of the SE with corrected line resistances are almost constant in the studied conditions. Thus, significant gain in SE accuracy can be achieved by correcting the transmission system model to actual conductor temperature.

V. CONCLUSIONS

- Changes of transmission line resistances due to temperature have non negligible impact on state estimation accuracy;
- The accuracy of the state estimation results can be improved if resistance of power transmission grid model is corrected to particular weather and loading conditions by the methods discussed in the paper;
- Practical implementation of the proposed approach is possible and justifiable as it allows more accurate allocation of the transmission losses, determines more accurately power flows and the network voltage profile.

VI. ACKNOWLEDGEMENTS

The authors gratefully acknowledge support and fruitful discussions with Mats Larsson, Ernst Scholtz and Reynaldo Nuqui from ABB Corporate Research centers. The input from Marek Zima, Atel Netz AG clarifying of some aspects of power markets is sincerely appreciated.

REFERENCES

- [1] F. Schweppe, J. Wildes, "Power System Static-State Estimation, Part I: Exact Model", *Power Apparatus and Systems, IEEE Transactions on*, Vol. PAS - 89, January 1970, Page(s):120 - 125;
- [2] P. Zarco, A.G. Exposito, "Power system parameter estimation: a survey", *Power Systems, IEEE Transactions on*, Volume 15, Iss. 1, Feb. 2000, Page(s):216 - 222;

- [3] K. Clements, R. Ringlee, "Treatment of parameter uncertainty in power system state estimation", *Power Apparatus and Systems, IEEE Transactions on*, July 1974;
- [4] A. Abur, A. G. Exposito, "Power System State Estimation: Theory and Implementation", Marcel Dekker, 2004.
- [5] Granino A. Korn and Theresa M. Korn, "Mathematical Handbook for Scientists and Engineers: Definitions, Theorems, and Formulas for Reference and Review", 2nd Rev, Dover Publications, June 2000;
- [6] W.A.Lewis, P. D. Tuttle, "The Resistance and Reactance of Aluminium Conductors, Steel Reinforced", *IEEE Transactions on Power Apparatus and Systems*, pp. 1189-1215, Feb. 1958.
- [7] *IEEE standard for Calculation the Current-Temperature Relationship of Bare Overhead Conductors*, IEEE Std 738-1993, 8 Nov 1993;
- [8] H. E. House, P. D. Tuttle, "Current carrying capacity of ACSR", *IEEE Transactions on Power Apparatus and Systems*, pp. 1169-1178, Feb. 1958.
- [9] IEEE systems description. Available at: <http://www.ee.washington.edu/research/pstca/>
- [10] V. T. Morgan, "Effects of alternating and direct current, power frequency, temperature, and tension on the electrical parameters of ACSR conductors", *Power Delivery, IEEE Transactions on*, Volume 18, Issue 3, July 2003 Page(s):859 - 866.
- [11] William D.Stevenson, *Elements of the Power System Analysis*, McGraw-Hill Book Company, 1962
- [12] Data services of Astronomical Applications Department of the U.S. Naval Observatory, Positions of Selected Celestial Objects. Available at: <http://aa.usno.navy.mil/data/docs/AltAz.html>
- [13] M.Weibel, W.Sattinger, P.Rothermann, U.Steinegger, M.Zima, G.Biedenbach, "Overhead Line Temperature Monitorig Pilot Project", *CIGRE 2006 Session*, SC B2-311, Paris, August 27 - September 1, 2006.
- [14] KEMA, Metrics for Determining the Impact of Phasor Measurements on Power System State Estimation, *Eastern Interconnection Phasor Project*, March 2006.

VII. BIOGRAPHIES



Marija Bockarjova graduated from the Riga Technical University, Latvia in 2002. She continued studies at the faculty of Electrical and Power Engineering as Ph.D. student and in 2000-2005 was a planning engineer at the national power company Latvenergo. In 2005 she started the Ph.D studies at ETH Zürich.



Göran Andersson (M'86, SM'91, F'97) was born in Malmö, Sweden. He obtained his M.S. and Ph.D. degree from the University of Lund in 1975 and 1980, respectively. In 1980 he joined ASEA:s, now ABB, HVDC division in Ludvika, Sweden, and in 1986 he was appointed full professor in electric power systems at the Royal Institute of Technology (KTH), Stockholm, Sweden. Since 2000 he is full professor in electric power systems at the Swiss Federal Institute of Technology (ETH), Zürich, where he heads the powers systems laboratory. His research interests are in power system analysis and control, in particular power systems dynamics and issues involving HVDC and other power electronics based equipment. He is a member of the Royal Swedish Academy of Engineering Sciences and Royal Swedish Academy of Sciences and a Fellow of IEEE.